Electronic supporting information for the article Local pH and effective $\mathrm{p}K_\mathrm{A}$ of weak polyelectrolytes – insights from computer simulations

Lucie Nová,* Filip Uhlík,† and Peter Košovan‡
Department of Physical and Macromolecular Chemistry, Faculty of Science, Charles University in Prague, Hlavova 8, 128 00 Praha 2, Czech Republic
(Dated: February 23, 2017)

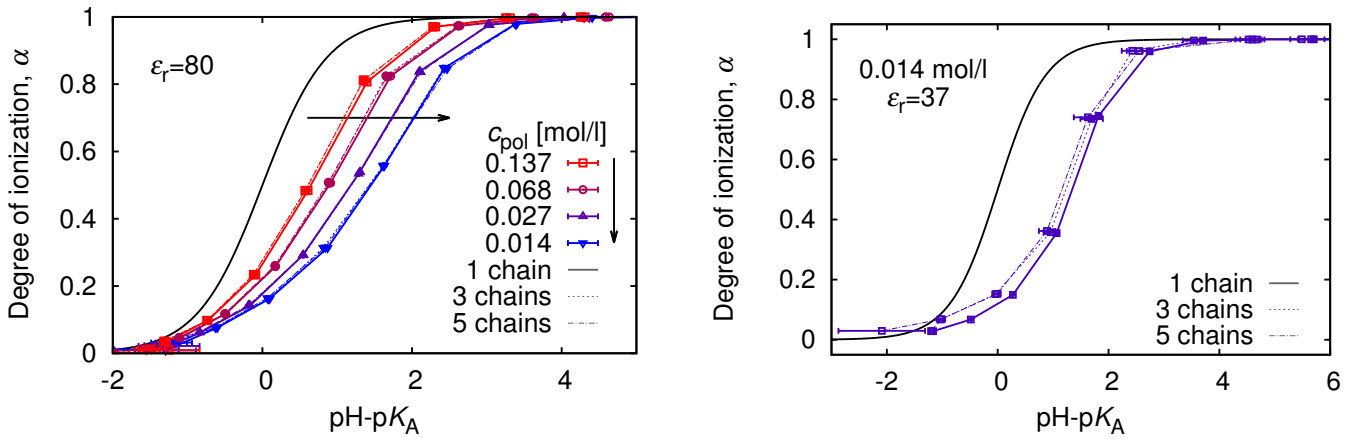

FIG. 1. The titration curves obtained with 1, 3 and 5 chains per simulation box at $\varepsilon_\mathrm{r} = 80$ (left) and $\varepsilon_\mathrm{r} = 37$ (right). At $\varepsilon_\mathrm{r} = 80$ the differences are minor, indicating that the finite-size effects due to a small number of chains are negligible. At $\varepsilon_\mathrm{r} = 37$ we observe more significant differences between 1 and 3 chains but almost no difference between 3 and 5 chains. In any case, these finite size effects are much smaller than the deviation from the ideal titration curve.

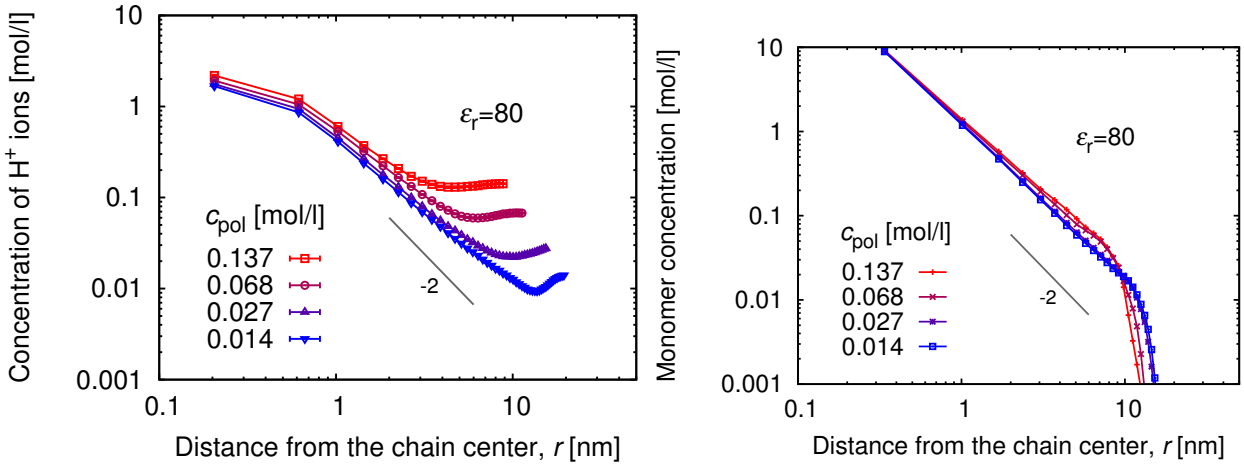

FIG. 2. Left: Proton concentration profiles obtained with 5 chains per simulation box for fully ionized weak polyelectrolytes with $K_\mathrm{A} = 10$, ($\alpha = 1$), solvent permittivity ε_r=80 and a series of polymer concentrations, c_pol.
Right: conentration profiles of polymer segments in the same systems.

* lucie.nova@natur.cuni.cz
† filip.uhlik@natur.cuni.cz
‡ peter.kosovan@natur.cuni.cz

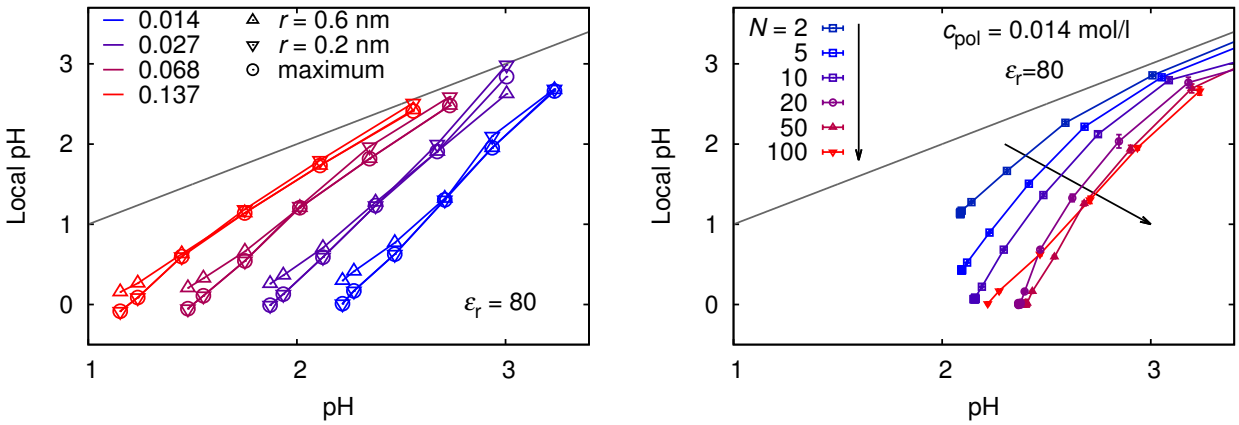

FIG. 3. Right: Sensitivity analysis, comparing results obtained with various definitions of local pH. Circles: local pH obtained from the maximum of the $c_{H^+}(r)$ dependence (our standard definition); Inverted and upright triangles: alternative definitions of local pH obtained from $c_{H^+}(r)$ at a fixed value of $r = 0.2\,\mathrm{nm}$ and $r = 0.6\,\mathrm{nm}$, respectively. These correspond to the first and second bin of the histogram used to determine $c_{H^+}(r)$. All curves display the same trends. The minor differences at the lowest pH values are inconsequential for the discussion and conclusions presented in the article. Note we used a histogram with bins of width $w = r_0 = 0.41\,\mathrm{nm}$, and each bin includes the interval $[r - w/2 : r + w/2]$. Therefore the occurrence of maximum in $c_{H^+}(r)$ at r smaller than the particle size is not unphysical.
Left: Local pH in the vicinity of the chain, as a function of pH in the bulk for various polymer chain lengths, N.

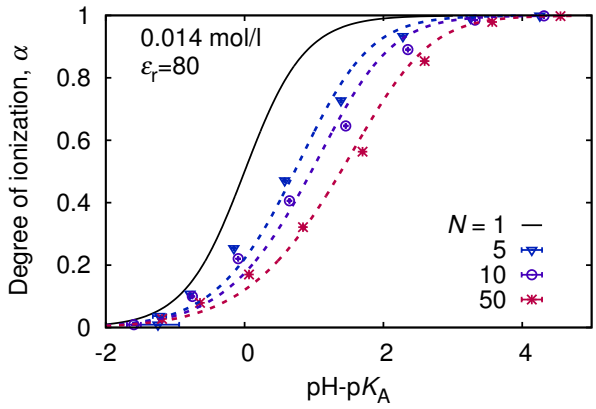

FIG. 4. The titration curves for different chain lengths compared to fits with the relation $\mathrm{p}K_{\mathrm{eff}} = \mathrm{p}K_{\mathrm{A}} + C\alpha^{1/3}$ with the constant C treated as adjustable parameter. The fit very well captures the simulation data for any chain length. However, the parameter values from the fit significantly differ from those that we obtained from the theory of Katchalsky and Gillis. [1]

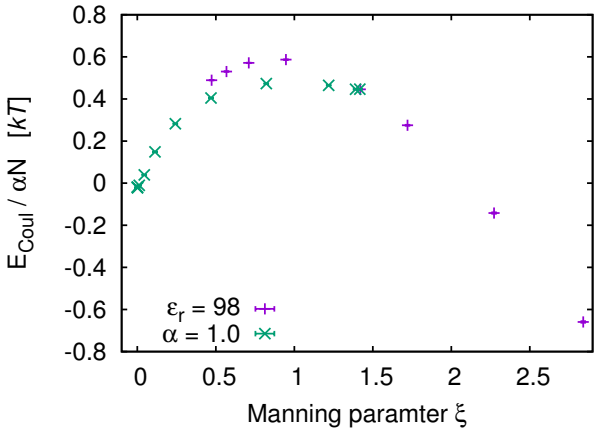

FIG. 5. Electrostatic energy per charged particle as a function of the Manning parameter for two selected systems: (i) fixed value of $\varepsilon_r = 98$ and a full range of available values of α; (ii) fixed $\alpha = 1.0$ and a full range of available values of ε_r. For an infinite homogeneously charged cylinder, such plot features a master curve with a cusp at $\xi = 1$, indicating second order transition. For our finite and flexible chains with inhomogeneously distributed point charges the transition is gradual and can be idendified by the changing sign of the derivative $\partial E/\partial\xi$ [2, 3].

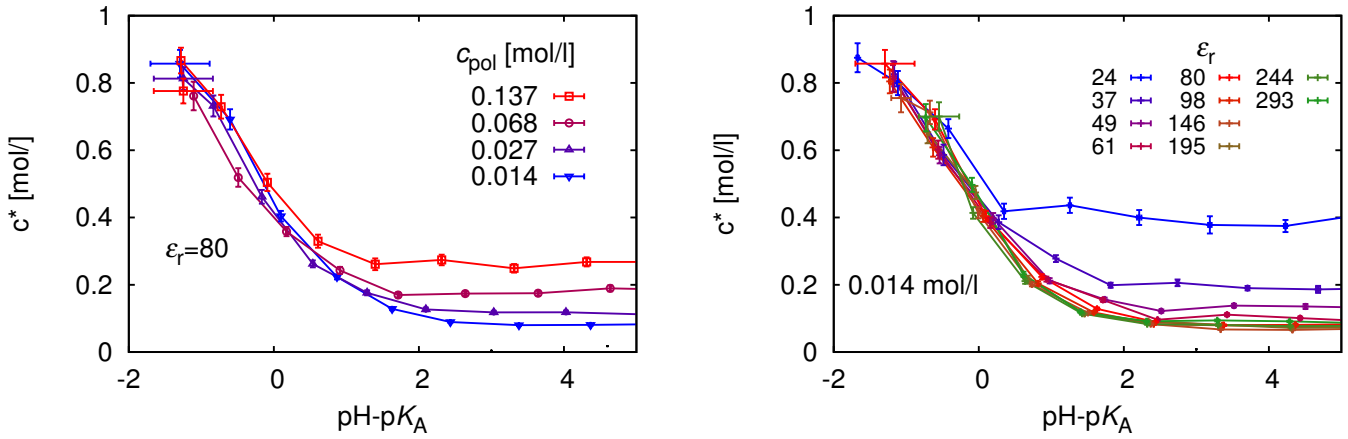

FIG. 6. Overlap concentration, c^* for different concentrations and permittivities. As the chain expands with increasing ionization, the value of c^* decreases almost by a factor of 10 as compared to the neutral chain.

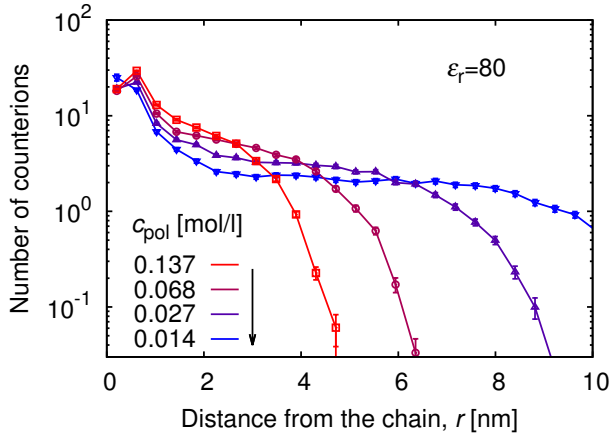

FIG. 7. Distribution of counterions along the polyelectrolyte chain at various polymer concentrations, $c_{\rm pol}$, at $\alpha \approx 1$. Note that the plateau is well developed only at the lowest concentration. Also note that in this figure we measure the distance to the nearest polymer chain, therefore the profile steeply drops as the distance approaches chain-chain separation, unlike Fig. 2.

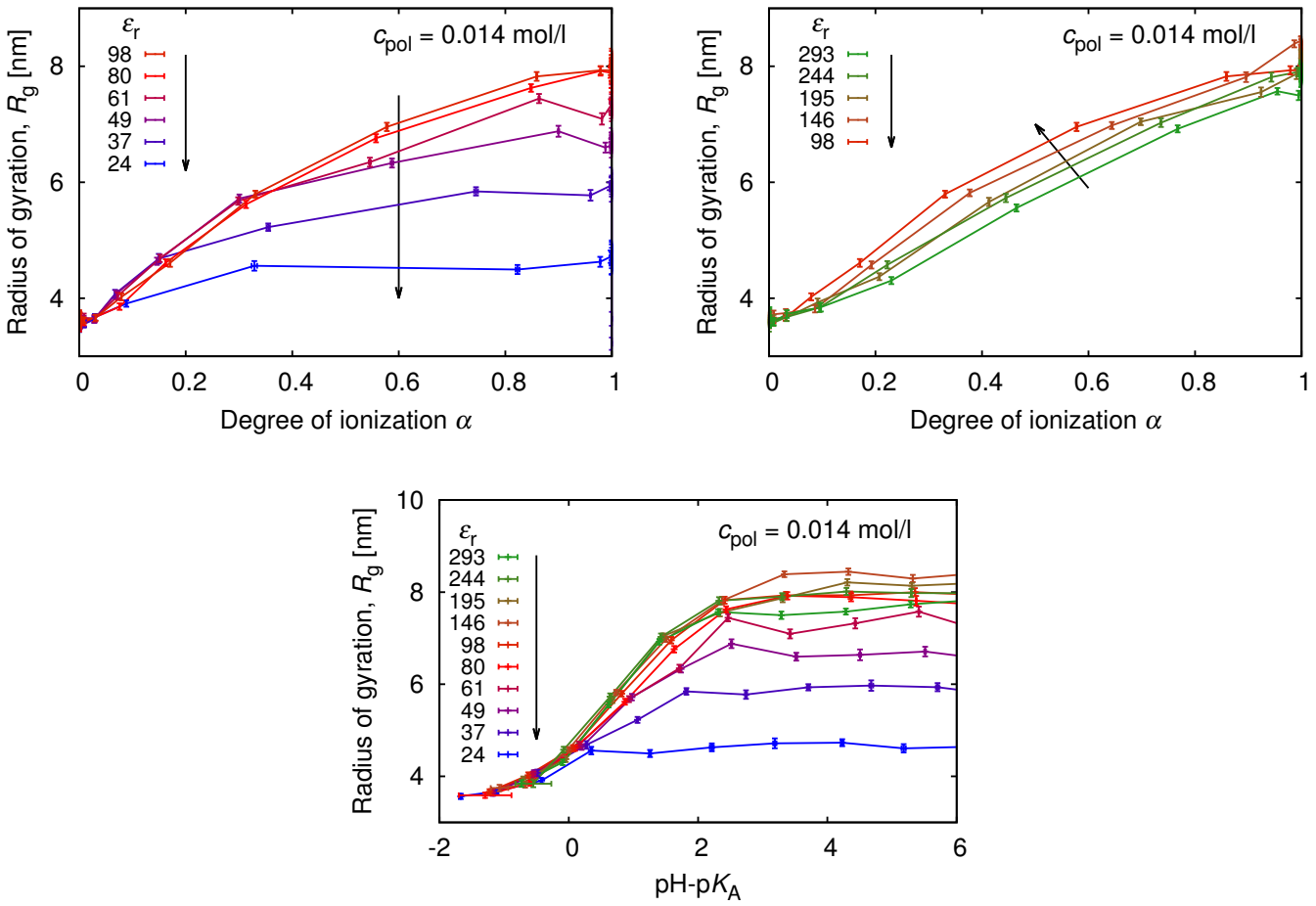

FIG. 8. Variation of radius of gyration, R_g, for various relative permittivities, ε_r. R_g first increases with decreasing ε_r, up to $\varepsilon_r \approx 80$, and then starts to decrease again as the ions start to condense on the chain and the cohesive energy of electrostatic interactions overwhelms the entropy loss.

[1] A. Katchalsky and J. Gillis. Theory of the potentiometric titration of polymeric acids. *Rec. Trav. Chim.*, 68(6):879, 1949.

[2] A. Naji and R. R. Netz. Counterions at charged cylinders: Criticality and universality beyond mean-field theory. *Physical Review Letters*, 95(18):185703, 2005.

[3] Ali Naji and Roland R. Netz. Scaling and universality in the counterion-condensation transition at charged cylinders. *Phys. Rev. E*, 73:056105, May 2006.

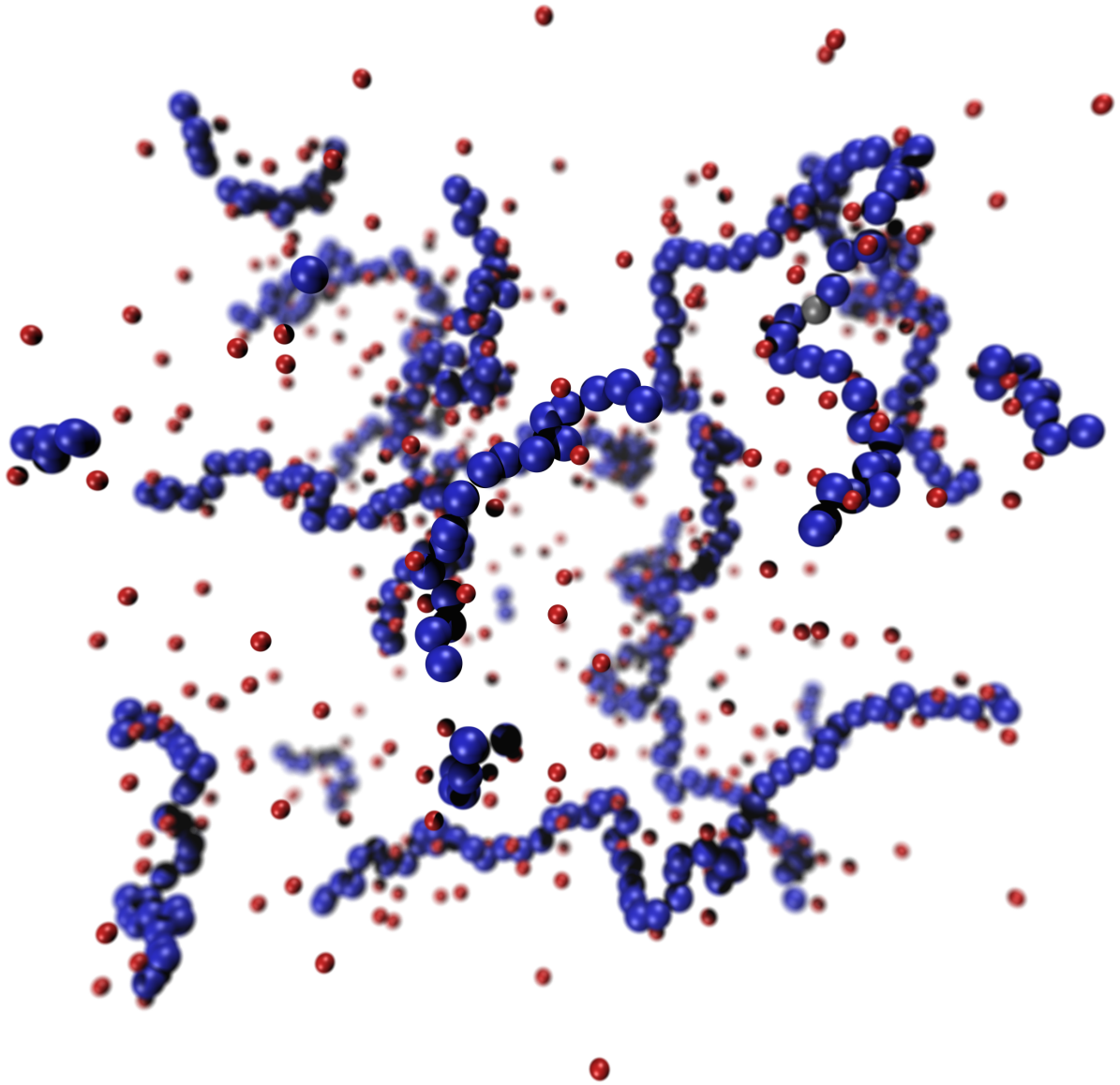

FIG. 9. Snapshot of the simulation box with 5 chains in the box for $\varepsilon_r \approx 80$, $c_{pol} \approx 0.137\,\mathrm{mol/l}$ and $\alpha \approx 1$. Colour code: silver – uncharged monomer, blue – charged monomer, red – H^+ ion.